Eur. Phys. J. B (2012) 85: 60
DOI: 10.1140/epjb/e2012-20958-8

THE EUROPEAN PHYSICAL JOURNAL B

Regular Article

Study of random sequential adsorption by means of the gradient method

E.S. Loscar[1,2,a], N. Guisoni[3], and E.V. Albano[2,3]

[1] Instituto de Investigaciones Fisicoquímicas Teóricas y Aplicadas (INIFTA), Facultad de Ciencias Exactas, Universidad Nacional de La Plata, CONICET CCT-La Plata, Sucursal 4, CC 16 (1900) La Plata, Argentina
[2] Departamento de Física, Facultad de Ciencias Exactas, Universidad Nacional de La Plata, La Plata, Argentina
[3] Instituto de Física de Líquidos y Sistemas Biológicos (IFLYSIB), Universidad Nacional de La Plata, CONICET CCT-La Plata; CC 565 (1900) La Plata, Argentina

Received 25 November 2011 / Received in final form 29 December 2011
Published online 13 February 2012 –

Abstract. By using the gradient method (GM) we study random sequential adsorption (RSA) processes in two dimensions under a gradient constraint that is imposed on the adsorption probability along one axis of the sample. The GM has previously been applied successfully to absorbing phase transitions (both first and second order), and also to the percolation transition. Now, we show that by using the GM the two transitions involved in RSA processes, namely percolation and jamming, can be studied simultaneously by means of the same set of simulations and by using the same theoretical background. For this purpose we theoretically derive the relevant scaling relationships for the RSA of monomers and we tested our analytical results by means of numerical simulations performed upon RSA of both monomers and dimers. We also show that two differently defined interfaces, which run in the direction perpendicular to the axis where the adsorption probability gradient is applied and separate the high-density (large-adsorption probability) and the low-density (low-adsorption probability) regimes, capture the main features of the jamming and percolation transitions, respectively. According to the GM, the scaling behaviour of those interfaces is governed by the roughness exponent $\alpha = 1/(1+\nu)$, where ν is the suitable correlation length exponent. Besides, we present and discuss in a brief overview some achievements of the GM as applied to different physical situations, including a comparison of the critical exponents determined in the present paper with those already published in the literature.

1 Introduction

The study and understanding of random sequential adsorption (RSA) processes have attracted large attention as paradigmatic approaches towards irreversibility, as well as due to the ubiquity of the phenomena in many fields of physics and chemistry. The main features of the RSA of objects on a sample are: (i) the adsorption is irreversible, so that desorption is no longer considered, (ii) both the adsorption position on the sample and the orientation of the object to be adsorbed are random events, and (iii) at any time only one object is being adsorbed, so that the process takes place sequentially. Of course, several variants of the RSA processes including, e.g. diffusion [1,2], relaxation [3,4] and dissociation [5,6] of the adsorbed particles, the competition between different species [7,8], as well as anisotropic sequential deposition [9], have already been studied. For reviews of RSA see e.g. [10,11].

By starting with an empty sample, at early stages RSA processes lead to the formation of small clusters of particles. Subsequently, one observes the growth of larger clusters and the onset of an incipient percolation cluster that spans over the whole sample, e.g. for $d > 1$ dimension [12]. So, just at the percolation threshold one observes a true geometrical second-order phase transition that belongs to the universality class of the standard percolation problem [12]. If the RSA process further continues, one may also observe the *jamming transition*, i.e. when there is no further space left on the sample for additional adsorption [10,11]. It is worth mentioning that along the present paper we use the term 'jamming' in order to identify the situation when no room is left for further adsorption on the sample. This is the usual practice in the RSA literature, in contrast to another use of this term in a wide variety of physical systems (granular media, colloidal suspensions, glasses, etc.) which may exhibit non-equilibrium transitions from a fluid-like to a solid-like state, characterized solely by the sudden arrest of their dynamics. In these cases, it is said that the jamming of the involved particles traps them kinetically, precluding further exploration of the phase space [13–15]. Within the context of RSA, the jamming density is no longer a trivial quantity

[a] e-mail: yasser.loscar@gmail.com

for the adsorption of dimers and larger particles. Both, percolation and jamming transitions are archetypal models studied by statistical physicists. However, interest in these topics spreads over many fields of science and technology such as condensed matter, physical chemistry, biology, etc. [10–12].

In a related context, the stationary state of a diffusion front of particles [16] can also be thought as an RSA experiment. In fact, by assuming a source (sink) of particles on the right-hand (left-hand) side of the sample, the density of particles decreases from 1 to 0 (from right to left) almost linearly along the direction of diffusion [16]. The main proposal of the present paper is that due to this gradient of density, one can simultaneously observe both a gradient percolation transition and a *gradient jamming transition*, which in turn can efficiently and straightforwardly be studied by means of the gradient method (GM) [17,18]. In the early studies of Sapoval et al. [16], the gradient percolation method was proved to be very useful to accurately locate the percolation threshold [19], as well as for the evaluation of some critical exponents of the percolation transition [16]. Very recently, we have generalised this method in order to study irreversible phase transitions (IPT's) [17,18], both of first and second order, occurring between absorbing and active states. By applying the new approach, i.e. the so-called GM, to the Ziff-Gulari-Barshad model for the catalytic oxidation of CO [17], and to the forest-fire model with immune trees [18], it has been shown that one can characterise both the absorbing phase transitions and the percolation transitions in a unified fashion. We also note that the GM allowed for the calculation of the critical exponents.

Within this context, the aim of this paper is to apply the GM to the RSA problem and show that both percolation and jamming can also be studied in a unified fashion by means of a single numerical simulation. For this purpose we apply a suitable version of the GM to the RSA of both monomers and dimers in a lattice in $d = 2$ dimensions. Basically, we perform RSA experiments where a density gradient is imposed along one direction of the sample, leading to the formation of percolation and jamming interfaces that can be treated by using the same theoretical background. It should be mentioned that previous standard studies of these transitions have already shown that they share several relevant characteristics [20,21]. However, one must keep in mind that the jamming process is not an actual thermodynamic transition. Along this paper, particular attention will be devoted to describe the scaling laws of the interface roughness and the corresponding exponents. This purpose will be achieved by means of the generalisation, in the case of RSA, of the relationships early developed by Sapoval et al. [16] for the percolation problem associated with a diffusion front. We will also show that the proposed approach yields accurate results with a minimal computational effort.

We have organised this paper according to the following schema: in Section 2 we provide the theoretical background of the GM, Section 3 is devoted to the description of the RSA gradient method and the simulation procedure. In Section 4 we first derive suitable scaling relationships for the RSA of monomers. Subsequently we apply the GM to the RSA of monomers and dimers, confirming the scaling schema already developed. Finally, we state our conclusions in Section 5.

2 The gradient method approach

The GM approach is based on the study of some suitable experiment or system in which a control parameter p varies monotonically along one spatial coordinate x ($0 \leq x \leq L_x$), where L_x is the system size in the x-direction. We assume this variation according to

$$p(x) = p_0 + (p_1 - p_0)x/L_x \tag{1}$$

where, for simplicity, we have taken constant gradient $\Delta = \nabla p = (p_1 - p_0)/L_x$, with $p_1 > p_0$.

Let us also assume the existence of a phase transition at the critical point $p \equiv p_c$ and, of course, that this point lies within the interval $[p_0, p_1]$, namely $p_0 < p_c < p_1$. Under this condition the GM naturally exhibits at least one interface between these coexisting phases. In fact, if $x_c \equiv X(p_c)$ is the coordinate given by equation (1), for $x > x_c$ (i.e. $p > p_c$) one has one phase (say phase A), while for $x < x_c$ (i.e. $p < p_c$) the second phase (say phase B) is present. It is worth mentioning that the GM does not provide a unique definition of the interface between phases A and B. Far from being a shortcoming, this is a powerful advantage of the GM because one can always define, locate, and calculate the properties of at least one suitable interface between phases A and B, capable of giving useful information on the phase transition occurring at $x_c = X(p_c)$.

In order to achieve a quantitative description of the physical situation, along this paper and following [17,18], we will determine and study the properties of two different interfaces, i.e. the so-called single-valued interface (SVI), and the multivalued interface (MVI). For the sake of clarity, it is convenient to state that our study will be performed in two dimensions by assuming a lattice in a rectangular geometry of sides $L_x \times L_y$, where the gradient is applied along the x-direction (rows), while the L_y-direction (columns) is parallel to the interfaces considered in the GM. The simplest definition corresponds to the SVI that is given by the set of points $\{a_j\}, j = 1, 2, \ldots L_y$ belonging to the phase A that are in contact with the phase B, but are located on the rightmost side of each row j. On the other hand, in order to construct the MVI one determines all the occupied sites in contact with the rightmost column of the sample. These sites, connected by means of nearest neighbours, are denoted as the 'land'. Also, empty sites are linked through both nearest- and next nearest-neighbour sites and form a large cluster that is termed the 'sea', connected with the leftmost column of the sample. The sites not connected with the two large clusters of land and sea are identified as 'islands' and 'lakes', respectively, but they are irrelevant. In fact, by definition, the MVI is given by the 'seashore' where 'land' and 'sea'

are in contact. In this way the number of points belonging to the MVI could be greater than L_y, which motivates the name of the multivalued interface, in contrast to the single-valued interface. For additional details on the definitions of the interfaces and the algorithms used to locate them see, e.g. [17,18].

Let $\mathrm{Int} = \{x_i\}, i = 1, 2, \ldots M$ be the set of coordinates corresponding to the sites belonging to a given interface between phases A and B. Here one has that $M = L_y$ and $M \geq L_y$ for the SVI and the MVI, respectively. The average position of the interface is given by

$$\langle x \rangle_{\mathrm{Int}} = \frac{1}{M} \sum_{\mathrm{Int}} x_i, \tag{2}$$

while the width W of the interface can be calculated as the rms deviation of $\langle x \rangle_{\mathrm{Int}}$, as usual. So,

$$W = \sqrt{\frac{1}{M} \sum_{\mathrm{Int}} (x_i - \langle x \rangle_{\mathrm{Int}})^2}. \tag{3}$$

On the other hand, after proper identification of the largest cluster associated with one phase, one can define the cluster density profile measured along the coordinate where the gradient is applied, namely $\rho_{\mathrm{cl}}(x, \Delta)$, which is just the density of the components of the cluster measured at each column of coordinate x. The function ρ_{cl} contains the most important information that one can obtain by using the GM, and establishes the link between the interfacial properties and the standard criticality observed at p_c. In fact the derivative of ρ_{cl} is a Gaussian-like function whose peak can be associated with the location of the interface according to $p_c \approx p(\langle x \rangle_{\mathrm{Int}})$ [16], while its width is of the order of the interface width W. In order to work out the scaling behaviour of the function $\rho_{\mathrm{cl}}(p, \Delta)$, it is useful to rewrite equations (2) and (3) as a function of the control parameter by using equation (1), that is

$$\langle p \rangle_{\mathrm{Int}} = \frac{1}{M} \sum_{\mathrm{Int}} p(x_i), \tag{4}$$

and

$$w = \sqrt{\frac{1}{M} \sum_{\mathrm{Int}} \left(p\left(x_i\right) - \langle p \rangle_{\mathrm{Int}}\right)^2}, \tag{5}$$

where it is worth stressing that W and w are measured in units of lattice spaces and control parameter units, respectively.

Now, if we assume that $p \equiv p_c$ is a critical point that has a diverging correlation length (ξ) given by

$$\xi \propto |p - p_c|^{-\nu}, \tag{6}$$

where ν is the correlation length exponent, it can be proved that the correlation length is related to the gradient according to [16]

$$\xi \propto |\Delta|^{-\frac{\nu}{\nu+1}}. \tag{7}$$

Coming back to the cluster density function $\rho_{\mathrm{cl}}(p, \Delta)$, it is clear that the critical behaviour appears in the limits $|p - p_c| \to 0$ and $\Delta \to 0$, where ρ_{cl} converges to the Heaviside step function. Therefore, by using equations (6) and (7) in these limits, the scaling relationship for ρ_{cl} becomes

$$\rho_{\mathrm{cl}}(p, \Delta) = \Psi\left(\left[p - p_c\right] \Delta^{-\frac{1}{\nu+1}}\right), \tag{8}$$

where Ψ is a suitable scaling function. It is worth recalling that equation (8) is of the same type as that of the percolation probability in the well known standard percolation problem [12]. So, one can prove that for $\Delta \to 0$ (but $\Delta \neq 0$), the width of the transition region (i.e. w, which is measured according to Eq. (5)) and the position of the effective critical point ($\langle p \rangle_{\mathrm{int}}$, as given by Eq. (4)), behave according to

$$w \propto \Delta^{\alpha}, \quad \alpha = \frac{1}{\nu + 1}, \tag{9}$$

and

$$\langle p \rangle_{\mathrm{Int}} - p_c \propto \Delta^{\alpha}, \quad \alpha = \frac{1}{\nu + 1}, \tag{10}$$

respectively, where α is the so called roughness exponent [22].

Furthermore, in the $\Delta \to 0$ limit, one can estimate the critical point p_c with high precision, by using equation (8), as the coordinate of the crossing point $\rho^* \equiv \rho_{\mathrm{cl}}(p_c, \Delta) \equiv \Psi(0)$ among curves of the cluster density corresponding to different values of Δ.

The relationships discussed previously have been used for the study of several models, with the gradient percolation transition as the paradigmatic case [16–18,23]. Here, we will show that the same schema can also be applied to RSA problems. For this purpose we shall exploit the similarity between percolation and jamming. In fact, by using the same adsorption experiment or simulation, we will show that the MVI is suitable to describe the critical properties of the percolation transition, while the SVI is related to the properties of the jamming transition. The similarity between jamming and percolation has also been observed before, when jamming has been used to measure the dimensionality of the samples [20,24–26]. For RSA problems, it is well known that the jamming transition is not actually a true phase transition, in the thermodynamic sense, and consequently it lacks a diverging correlation length. In this case, correlations between particles are short-ranged and extend over few lattice units. Furthermore, the exponent ν_{J}, which plays the role of the correlation length exponent, can be calculated exactly and is given by [24,25]

$$\nu_{\mathrm{J}} = 2d/(2 + d_{\mathrm{f}}), \tag{11}$$

where d is the dimension of the substrate and d_{f} is the dimension of the active sites where the actual adsorption process takes place. Notice that equation (11) is quite general and also holds for a fractal set of active sites.

Along the next sections of the paper we will show that the previous discussions can be applied to the RSA of

monomers and dimers. We will propose a numerical version of the GM for RSA. After that we will show that the simplest case of jamming of monomers can be solved analytically and the scaling function can be found explicitly in the thermodynamic limit. Furthermore, focusing our attention on both the percolation and the jamming transitions, we will study RSA processes of both dimers and monomers by means of extensive numerical simulations.

3 The gradient method applied to RSA and the numerical simulation schema

Our aim is to extend the recently proposed GM [17,18] to the study of RSA processes. The GM is inspired in the seminal work of Sapoval et al. [16] on the diffusion front (DF) problem, where the DF is originated by the diffusion of particles between a source and a sink, which are placed at the rightmost and leftmost sides of a sample, respectively. In the DF problem, the relevant parameter is the density of diffusing particles that monotonically decreases from the source towards the sink, i.e. a concentration gradient is naturally established as a consequence of random motion and excluded volume, which fully satisfies the equation of diffusion. Furthermore, it is well known that the established gradient is almost linear along the source-sink direction, provided that the distance between them is large enough.

We propose that a similar concentration gradient can be generated in an RSA process just by assuming some constraint over the density of the adsorbed particles along a given direction, i.e. the gradient direction. In the standard notation of the RSA literature, the density of the adsorbed particles is the coverage θ. Now, for the RSA case one has to use the constraint coverage as the control parameter p as is used in Section 2, that is $\theta \to p$.

The above-mentioned constraint, which is suitable for the implementation of an RSA process in a gradient, is called the linear constraint and it is implemented as follows: simulations are performed in two dimensions by assuming a lattice in a rectangular geometry of sides $L_x \times L_y$, where the gradient is applied along the x-direction, while the L_y-direction is parallel to the interfaces considered in the GM. For the purpose of the simulations, periodic boundary conditions are applied along the L_y-direction, while the remaining boundaries along the L_x-direction are closed. In order to implement the RSA with the linear cut-off constraint, the density of each ith column ($1 \leq i \leq L_x$) cannot exceed i/L_x in order to satisfy $\theta(i) = \theta_0 + (\theta_1 - \theta_0)i/L_x$, which for the RSA problem is equivalent to equation (1), with $\theta_1 = 1$ and $\theta_0 = 0$. For the case of the RSA of monomers a column i is selected at random with probability $1/L_x$. Then, if the density of the column is smaller than i/L_x, a site from this column is selected at random with probability $1/L_y$ and the adsorption of a particle is considered provided that the selected site is empty. The RSA continues until particles can no longer be adsorbed on any place of the sample due to the linear cut-off constraint.

In order to implement the RSA of dimers under the linear cut-off constraint, one also selects at random a column with probability $1/L_x$ and subsequently a site belonging to that column with probability $1/L_y$. However, since now one requires an additional site for the adsorption process, a neighbouring site of the previously selected one is also chosen at random with probability 1/4. Notice that this additional site may lie on the same column as that of the first one (with probability 1/2) undergoing the same constraint, or it may be located in two adjacent columns (with probability 1/4 on each side of the originally selected column), so that in that latter case it may undergone a slightly different constraint. We have checked that our results (see below) are independent of this detail, as expected since a correction of the order of $1/L_x$ is involved. So, adsorption of the dimer is accepted provided that both selected sites are vacant and that the linear cut-off constraint of the first selected site is satisfied. The RSA process stops when no sites for further adsorption of dimers are left on the sample.

4 Results and discussion

4.1 The GM applied to the RSA of monomers

For this case one recovers the standard DF problem, early studied by Sapoval et al. [16], so we will only discuss the main results focusing our attention on the properties of the SVI that capture the behaviour of the jamming transition. Then, those results corresponding to the MVI that capture the behaviour of the standard percolation problem, already discussed in terms of the DF problem [16], will only be briefly mentioned.

We consider a two-dimensional lattice in a stationary DF configuration. This means that the density of monomers, in the horizontal direction, varies linearly from $\theta = 0$ (on the left) to $\theta = 1$ (on the right).

Let us now point our attention to any row in this simple configuration. In order to simplify the formulation of the following equations, we label the sites of a given row with the horizontal coordinate (i.e. its column number) as $i' = 0, \ldots, L_x - 1$, from right to left (i.e. being i the previously used index, one has $i' = L_x - i$). The occupation probability, for a site with label i', will be $r(i') = 1 - i'/L_x$ and the probability to be empty, $q(i') = i'/L_x$. The gradient in the density is simply given by $\Delta = 1/L_x$. Furthermore, for a given row, the site belonging to the SVI interface can be taken as $i' = I$ if all sites with coordinate i', so that $i' < I$, are occupied, and the I-site itself is empty[1]. Then, the probability that a site i' of a given

[1] There is an uncertainty of the order of $1/L_x = \Delta$ in the definition of this location because the coordinates of the sites are integer numbers, whilst the coordinate of the resulting interface calculated according to equation (2) can be a real number. Despite this shortcoming any choice must lead to the same result in the limit $\Delta \to 0$. So, the error in the GM is of the order of $\Delta/2$.

row belongs to the SVI is given by

$$p(i' = I, L_x) = r(0)r(1)r(2)\dots r(I-1)q(I) = \frac{I\ L_x!}{L_x^{I+1}(L_x - I)!}. \quad (12)$$

By considering the whole lattice, equation (12) gives us the horizontal distribution of the sites belonging to the SVI. By taking L_x large enough and by using the Stirling formula for the factorial numbers, it is easy to show that $p(I, L_x)$ can be expressed as a function of the new variable $z = I/L_x$, with $0 \leqslant z < 1$, as

$$p(z, L_x) \propto z e^{-L_x \psi(z)}, \quad (13)$$

where the function ψ is given by

$$\psi(z) = z + (1-z)\ln(1-z), \quad (14)$$

which is a monotonically increasing function and its minimum is $\psi(z = 0) = 0$. From equation (13) one can see that for large enough L_x, only that minimum gives the leading behaviour of p. Then, by making a Taylor expansion of ψ around $z = 0$, we conclude that

$$p(z, \Delta) \propto\ z \exp\left[-\frac{z^2}{2\Delta}\right], \quad (15)$$

where we used $\Delta = 1/L_x$. The solid cluster of the jammed state, which is placed on the right-hand side of the SVI, is compact in the sense that it lacks holes, and its cluster density $\rho_{\rm cl}(z, \Delta)$ can be calculated as

$$\rho_{\rm cl}(z, \Delta) = -\int_1^z p\,(z', \Delta)\, dz'. \quad (16)$$

Because the maximum of $\rho_{\rm cl}(z, \Delta)$ is $\rho^{max} = 1$, one has

$$\rho_{\rm cl}(z, \Delta) = \exp\left[-\frac{z^2}{2\Delta}\right]. \quad (17)$$

The coordinate $z_c(\Delta)$ that measures the position of the interface and the width corresponding to the jamming transition can now be obtained straightforwardly. In fact, from equation (15) and identifying z_c with the maximum of $p(z, \Delta)$, one obtains

$$z_c(\Delta) = z_c(0) + \Delta^{1/2}, \quad (18)$$

where $z_c(0) = z_c(\Delta \to\ 0) = 0$. Also, the width of the transition ($w_{\rm SVI}$), given by the characteristic width of the exponential function (Eq. (17)), is

$$w_{\rm SVI} = \Delta^{1/2}. \quad (19)$$

Now physically, the relevant variable is the coverage, $\theta = 1 - z$, therefore we can explicitly write the scaling relationship introduced in Section 2 (Eq. (8)) just by using equation (17), namely

$$\rho_{\rm cl}(\theta, \Delta) = \Psi\left(\left[\theta - \theta_{\rm J}^{\rm M}\right]\Delta^{-1/2}\right), \quad (20)$$

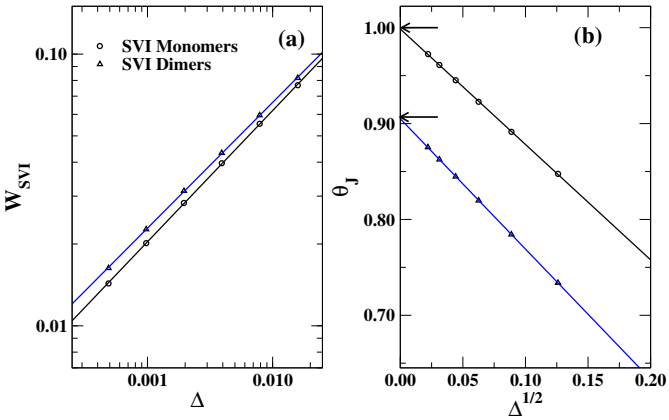

Fig. 1. (Color online) RSA of monomers (circles) and dimers (triangles) under the linear gradient constraint. (a) Log-log plots of the width of the SVI versus the gradient Δ. The continuous lines are power-law fits and the resulting exponents are $\alpha_{\rm J} = 0.48 \pm 0.02$ ($\alpha_{\rm J} = 0.46 \pm 0.02$) for the SVI corresponding to the adsorption of monomers (dimers). (b) The position of the SVI is shown versus $\Delta^{1/2}$, as obtained for different gradients. The continuous lines are linear fits, so that the intersections with the vertical axis are the extrapolated jamming coverages $\theta_{\rm J}$. The arrows indicate the coverage for the jamming transition $\theta_{\rm J}^{\rm M} = 1$ ($\theta_{\rm J}^{\rm D} \approx 0.907$) for monomers (dimers). More details in the text.

where the critical (jamming) coverage is $\theta_{\rm J}^{\rm M} = 1$ and the scaling function is $\Psi(u) = e^{-\frac{u^2}{2}}$.

In order to test the above-developed theoretical framework, we simulated the RSA of monomers under the gradient constraint. Figure 1a shows a log-log plot of the width of the SVI ($w_{\rm SVI}$) given by equation (5) versus the gradient Δ, as obtained for square samples of different sizes ($64 \leq L_x \leq 2048$) that actually set the gradient. For the case of monomers, a power-law fit of the data to equation (9) yields $\alpha_{\rm J} = 0.48 \pm 0.02$, which is consistent with the exact theoretical value $\alpha_{\rm J} = 1/2$ given by equation (19). Figure 1b shows the location of the SVI, $\theta_{\rm J} \equiv \langle\theta\rangle_{\rm Int}$, as measured in units of the coverage by using equation (4), plotted as a function of $\Delta^{1/2}$. In this way, equation (10) is fully confirmed, and again the exactly obtained theoretical exponent $\alpha_{\rm J} = 1/2$ is verified for the case of monomers. On the other hand, the extrapolation of the data yields to the $\Delta \to\ 0$ limit $\theta_{\rm J}^{\rm M} = 0.999 \pm 0.005$. Also, we obtained $A = -1.21 \pm 0.02$ for the constant involved in equation (10).

Figure 2a shows plots of the density of the compact cluster located on the right-hand side of the SVI, which corresponds to the cluster of the jammed state ($\rho_{\rm cl}^{\rm SVI}$), as measured from the simulations, versus the control parameter $\theta(x)$ of each column of the sample. Results are obtained for different gradients that can be accomplished by taking samples of different lattice width L_x. In this case the crossing point between all the curves is trivially given by $\theta_{\rm J}^{\rm M} = 1$. Then by using the scaling relationship given by equation (8) with $p_c \equiv \theta_{\rm J}^{\rm M} = 1$ and $\nu_{\rm J} = 1$ (which corresponds to $\alpha_{\rm J} = 1/2$), one obtains an excellent

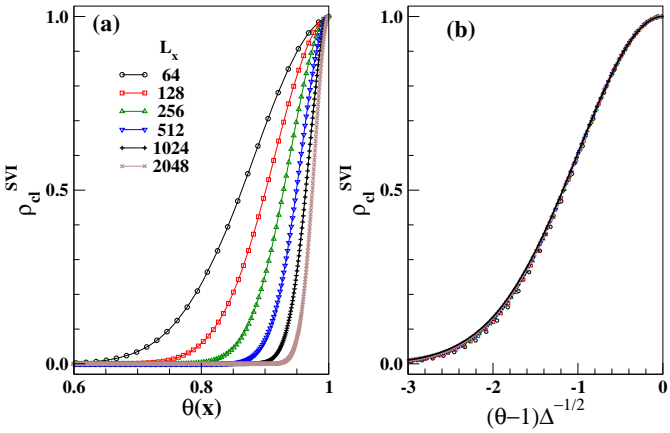

Fig. 2. (Color online) RSA of monomers under the linear gradient constraint. These data correspond to the same simulation used in Figure 1. (a) Plots of the density of the cluster defined by the SVI versus the parameter $\theta(x)$ as obtained for different lattice sizes (i.e. different gradients). Note the trivial intersection of the curves at $\theta_{\rm J}^{\rm M} = 1$. (b) Collapse of the data already shown in (a) obtained by rescaling the horizontal axis according to $(\theta - 1)\Delta^{-1/2}$. The continuous line is the theoretical scaling function (Eq. (20)) that is plotted without any adjusted parameter.

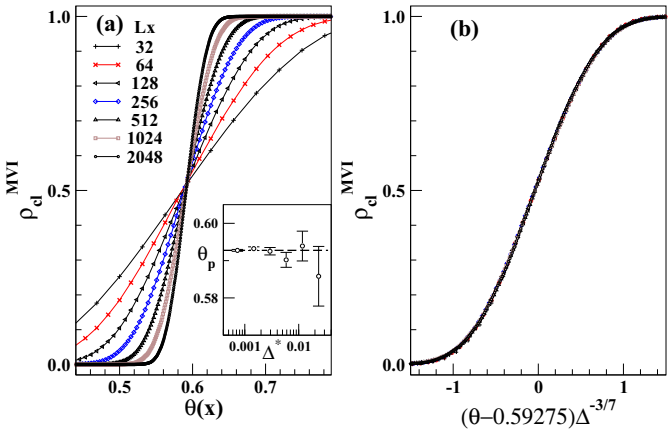

Fig. 3. (Color online) RSA of monomers under the linear gradient constraint. (a) Plots of the density of the percolation cluster defined by the MVI versus the control parameter $\theta(x)$ as obtained for different lattice sizes (i.e. different gradients). The inset shows plots of the intersection points between adjacent curves (shown in the same panel) against average values taken between consecutive gradients (Δ_1 and Δ_2), namely $\Delta^* \equiv (\Delta_1 + \Delta_2)/2$, which give us $\theta_{\rm p}^{\rm M} = 0.59274 \pm 0.00025$, that nicely converges towards the percolation threshold $\theta_{\rm p}^{\rm M} \simeq 0.59275$, shown as a dashed line. (b) Collapse of the data already shown in (a) obtained by rescaling the horizontal axis according to $(\theta - 0.59275)\Delta^{-3/7}$. More details in the text.

data collapse, as shown in Figure 2b. The continuous line in Figure 2b is the theoretical scaling function (Eq. (20)) derived above (without any adjusted parameter). So, the excellent agreement fully supports the previous theoretical treatment.

The previous results suggest that, although it is well known that the jamming transition is not actually a true phase transition, the exponent $\nu_{\rm J}$ given by equation (11) can be used as the correlation length exponent in equations (9) and (10). That is taking $d_{\rm f} = d = 2$ in equation (11), one gets $\nu_{\rm J} = 1$, and by inserting this figure in equations (9) and (10) one obtains $\alpha_{\rm J} = 1/2$ for the roughness exponent, in agreement with all of our previously discussed results.

An additional advantage of the GM is that by means of the same simulation results, the analysis of the MVI can also be used to gain insight into the standard percolation transition. In fact, the RSA of monomers in the GM maps onto the DF problem and consequently onto the percolation system as well. The power-law fit of the width of the MVI ($w_{\rm MVI}$) versus the gradient as obtained by performing simulations of the RSA of monomers (see Eqs. (5) and (9)) yields $\alpha_{\rm p} = 0.40 \pm 0.01$ (not shown here for the sake of space), i.e. a figure that slightly underestimates the exact value that can be obtained with the aid of equation (9) taking $\nu = 4/3$ for the standard percolation problem, namely $\alpha_{\rm p} = 3/7 \simeq 0.4286$. The observed discrepancy is due to the operation of strong finite-size effects. In fact, by using this type of measurement one has to evaluate local exponents, defined between two adjacent values of the gradient, and the exact value is recovered when these local exponents are properly extrapolated to the thermodynamic limit [18,27,28]. For a detailed discussion and application of the above procedure with the GM see [18]. Here, we will only quote that by considering the discussed correction, we obtained $\alpha_{\rm p} = 0.425 \pm 0.004$.

On the other hand, the massive percolation cluster is composed of sites belonging to the land and the lakes and islands inside the land. Figure 3a shows the density profiles associated with that massive percolation cluster plotted versus the coverage. It exhibits a common intersection point for different values of the gradient. The inset of Figure 3a shows the location of the intersection point between two curves of consecutive gradient values versus the averaged gradient. One has that these intersections converge towards the percolation threshold of the standard percolation problem, namely $\theta_{\rm p}^{\rm M} \simeq 0.59275$ [29], as expected. The percolation threshold can also be determined by using the position of the MVI (similar to Fig. 1b for the MVI) as was done before for the case of the DF problem by Sapoval et al. [16]. Also, by using the proposed scaling relationship for the density profile (Eq. (8)) one obtains an excellent data collapse of the results shown in Figure 3a, as depicted in Figure 3b. So far, we conclude that the RSA of monomers with the gradient constraint can be used to study both the jamming and the percolation transition in a unified fashion.

4.2 Application of the GM to the RSA of dimers

Let us now discuss the results corresponding to the RSA of dimers with the gradient constraint. Figure 1a shows a log-log plot of the width of the SVI ($w_{\rm SVI}$) versus the gradient. By fitting the obtained results with the aid of equation (9)

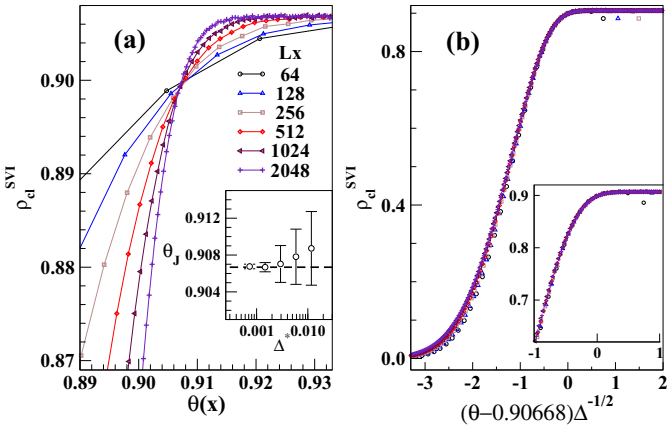

Fig. 4. (Color online) RSA of dimers under the linear gradient constraint. (a) Plots of the density of the cluster defined by the SVI versus the control parameter θ, as obtained for different lattice sizes (i.e. different gradients). The inset shows the intersection points between different (but consecutive) curves against average values taken between consecutive gradients (Δ_1 and Δ_2), namely $\Delta^* \equiv (\Delta_1 + \Delta_2)/2$, which converge to $\theta_J^D = 0.90676 \pm 0.00025$. The dashed line is the best known estimated value, taken from [9,10]. (b) Collapse of the data already shown in (a) as obtained by rescaling the horizontal axis according to $(\theta - 0.90668)\Delta^{-1/2}$. The inset is a zoom of the scaling region, i.e. $\theta \simeq \theta_J^D$, which shows the high quality of the data collapse. More details in the text.

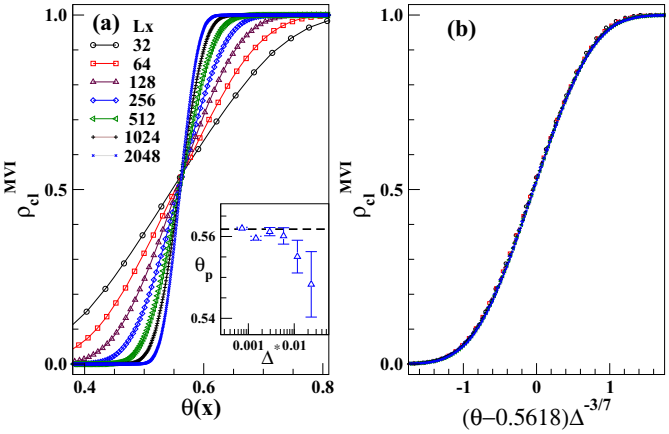

Fig. 5. (Color online) RSA of dimers under the linear gradient constraint. (a) Plots of the density of the percolation cluster defined by the MVI versus the control parameter $\theta(x)$ as obtained for different lattice sizes (i.e. different gradients). The inset shows plots of the intersection points between different (but consecutive) curves against average values taken between consecutive gradients (Δ_1 and Δ_2), namely $\Delta^* \equiv (\Delta_1 + \Delta_2)/2$, which converge to $\theta_p^D = 0.5620 \pm 0.0007$. The dashed line is the best known estimated value, taken from [9,10]. (b) Collapse of the data already shown in (a) as obtained by rescaling the horizontal axis according to $(\theta - 0.5618)\Delta^{-3/7}$.

for the case of dimers, one obtains $\alpha_J = 0.46 \pm 0.02$, i.e. a figure that is close to the exact value, namely $\alpha_J = 1/2$. The rather small difference between the exact value and the numerical determination could be due to the operation of finite-size scaling corrections, which would be more important for the case of the RSA of large objects, e.g. dimers, trimers, k-mers, etc., as compared with monomers where we have a good agreement with the theoretical value. In fact, by using the corrections discussed in [18] we obtained $\alpha_J = 0.495 \pm 0.008$, in excellent agreement with the expected value.

On the other hand, the location of the SVI (measured in units of θ) versus Δ yields a remarkable straightline (Fig. 1b) that, according to equation (10), extrapolates to the jamming coverage of dimers in the thermodynamic limit, namely $\theta_J^D = 0.905 \pm 0.005$, in good agreement with the best available value given by $\theta_J^D = 0.90668$ [9,10]. This result also supports our choice of $\alpha_J = 1/2$, as already discussed for the jamming transition by using $\nu_J = 1$ in equations (9) and (10).

Furthermore, plots of the density profiles of the clusters associated with the SVI versus θ (see Fig. 4a) exhibit a common intersection point close to θ_J^D, i.e. the jamming coverage for the RSA of dimers. Again, the extrapolation of the intersection points between curves measured for consecutive gradients (see the inset of Fig. 4a) converges towards $\theta_J^D = 0.90668$ (our estimate is $\theta_J^D = 0.90676 \pm 0.00025$). The data shown in Figure 4a, obtained for different gradients, can nicely be collapsed in a single curve just by using the proposed scaling relationship (Eq. (8)) with $p_c \equiv \theta_J^D = 0.90668$ and $\nu_J = 1$ (which corresponds to $\alpha_J = 1/2$), as shown in Figure 4b.

On the other hand, as already discussed, the percolation properties of the RSA process in the gradient method can be captured by analysing the MVI. Figure 5a shows plots of the densities of the percolation clusters defined by MVI versus the control parameter θ, as obtained for different gradients. The inset of Figure 5a shows a plot of the intersection points, as measured for consecutive gradients, which extrapolate to the value $\theta_p^D = 0.5620 \pm 0.0007$, in excellent agreement with an already known value for the percolation threshold of dimers $\theta_p^D = 0.5618 \pm 0.0001$ [9,20,30–32]. Also, Figure 5b shows the collapse of the curves already shown in Figure 5a according to equation (8) and obtained by assuming the exponent $\alpha_p = 1/(1+\nu) = 3/7$, where the value of α is evaluated by taking $\nu = 4/3$ for the standard percolation problem. Also, we measured the exponent α_p (not shown here for the sake of space) for the case of the MVI in the dimer gradient adsorption process by using the relationship given by equation (9) and the resulting estimated value is $\alpha_p = 0.41 \pm 0.01$. Again, with the corrections due to finite-size effects [18] we obtained $\alpha_p = 0.43 \pm 0.02$, in excellent agreement with the exact value $\alpha_p = 3/7 \simeq 0.4286$.

5 Conclusions

The gradient method (GM), inspired in the gradient percolation problem early studied in the context of the diffusion front of particles by Sapoval et al. [16], has previously

Table 1. Summary of critical exponents and critical points obtained by applying the Gradient Method. MVI and SVI refer to the multivalued and the single-valued interfaces defined in the text. ZGB = Ziff-Gulari-Barshad model for the monomer-dimer reaction [33]. FFMI = forest-fire model with immune trees (here we show only results for $p = 0.5$, for the complete results see [18]). KPZ = Kardar-Parisi-Zhang [22]. EW = Edwards-Wilkinson [22]. DF = Diffusion Front. RSA = Random Sequential Adsorption of dimers. GAP = Gradient Allee Process [23]. The exponent α is the roughness exponent of the interface and ν is the spatial correlation length exponent. In the last four columns we quote the exponents α measured by performing simulations and using equation (9) (the symbol * indicates values with finite-size scale corrections [18]), the critical parameters corresponding to each transition, the estimations of values of the critical parameters as obtained from the GM, and the available critical parameters found in the literature. The symbol † refers to results obtained in this paper. More details in the text.

Transition	Model	Interface	ν	$\alpha = \frac{1}{1+\nu}$	α	p_c	GM	Other methods
Standard Percolation	ZGB [17]	MVI	4/3 [12]	3/7 ≈ 0.4286	0.36(4)	P_{ox}^{MVI}	0.51(1)	0.515(15) [36]
	FFMI [18]				0.427(1)*	g_p	0.3470(2)	
	DF†				0.425(4)*	θ_p^M	0.59274(25)	0.59274602(4) [29]
	RSA†				0.43(2)*	θ_p^D	0.5620(7)	0.5618(1) [9]
Directed Percolation	ZGB [17]	SVI	0.733 [34,35]	0.577	0.56(2)	P_{ox}^1	0.3880(8)	0.3874 [37]
	FFMI [18]				0.577(4)*	g_c	0.5613(8)	0.5614 [38]
First-order (absorbing)	ZGB [17]	SVI/MVI	2/5 (KPZ) [22]	5/7 ≈ 0.7143	0.68(2)	P_{co}^2	0.5253(5)	0.52561 [39]
	GAP [23]	MVI	0.35 (EW) [22]	0.7407	0.74(1)			
Jamming	DF†	SVI	1 [24,25]	1/2	0.48(2)	θ_J^M	0.999(5)	1
	RSA†				0.495(8)*	θ_J^D	0.90676(25)	0.90668 [9]

been applied successfully to study absorbing phase transitions (both first and second order) and the percolation transition [17,18,23]. In this way, in our previous work we showed that with the aid of a single-valued interface (SVI) one is able to characterise active-inactive transitions (no matter the order of the transition), whereas with the aid of the multivalued interface (MVI) one can characterise the critical (geometrical) percolation transition.

In this work we proposed a new application of the GM for the case of RSA processes under a gradient constraint. We show that by using the GM the two transitions involved in the RSA process, namely percolation and jamming, can be studied simultaneously by means of the same set of simulations and by using the same theoretical background. In this way, the SVI and the MVI capture the main features of the jamming and percolation transitions, respectively. As in the case of absorbing phase transitions, the scaling behaviour of both interfaces is governed by the roughness exponent $\alpha = 1/(1+\nu)$, where ν is the suitable correlation length exponent [17,18]. For the case of the two-dimensional RSA studied in the present work we find that, for the jamming transition, the exponent that plays the role of the correlation length exponent is $\nu_J = 1$, which give us $\alpha_J = 1/2$ for the roughness exponent. This value is given by the relationship $\nu_J = 2d/(2+d_f)$, where d is the dimension of the substrate and d_f is the (fractal) dimension of the active sites where the actual adsorption process takes place, which has been calculated exactly before in the RSA context [24,25]. For the percolation transition one has $\nu = 4/3$, that is the critical exponent of the correlation length for the standard percolation transition [12], which gives $\alpha_p = 3/7 \simeq 0.4286$. The exponent $\alpha_J = 1/2$ was also derived theoretically for the RSA of monomers (see Eq. (19)). We also tested our analytical results by means of numerical simulations performed upon adsorption of monomers and dimers. For the case of the jamming transition we obtained $\alpha_J = 0.48 \pm 0.02$ (monomers) and $\alpha_J = 0.495 \pm 0.008$ (dimers) and for the standard percolation transition we obtained $\alpha_p = 0.425 \pm 0.004$ (monomers) and $\alpha_p = 0.43 \pm 0.02$ (dimers), all of them in excellent agreement with the theoretical predictions.

Let us also recall that the transition points are also determined with great accuracy by the GM. For the RSA of dimers we obtained the critical (jamming) coverage $\theta_J^D = 0.90676 \pm 0.00025$ (see Fig. 4), in good agreement with the best available value given by $\theta_J^D = 0.90668$ [9,10]. On the other hand, the percolation threshold of dimers obtained with the GM is $\theta_p^D = 0.5620 \pm 0.0007$ (see Fig. 5), in excellent agreement with an already known value, $\theta_p^D = 0.5618 \pm 0.0001$ [9,20,30–32]. For the RSA of monomers, the critical (jamming) coverage is the trivial value $\theta_J^M = 1$ and the coverage at the percolation threshold is $\theta_p^M \equiv p_c = 0.59275$ [29] since one recovers the DF problem. The value $\theta_J^M = 1$ is found analytically (Eq. (18)) and from the simulations we obtain an excellent agreement with the known values: $\theta_J^M = 0.999 \pm 0.005$ (Fig. 1b) and $\theta_p^M = 0.59274 \pm 0.00025$ (Fig. 3).

In order to provide a quick overview of some recent achievements of the GM as applied to different physical situations, Table 1 summarises the available results so far, including a comparison of the critical exponents obtained by using the GM with those already calculated exactly, or by means of different numerical approaches. We can see that the MVI is the meaningful interface in order to study the standard percolation transition, whereas the SVI is useful to study both absorbing phase transitions (first and second order) and the jamming transition. For the case of a first-order transition, when the density of the absorbing phase is greater than the threshold of the percolation transition, the differences between these two types of interfaces are washed out, and both the MVI and the SVI are completely equivalent, so that one has something like a

first-order percolation transition. This is precisely the case of the first-order irreversible phase transition of the ZGB model, whose interface behaviour (MVI/SVI) is given by the Kardar-Parisi-Zhang (KPZ) universality class, with $\nu_\perp = 2/5$ [22] and $\alpha_{\rm KPZ} = 5/7 \approx 0.7143$ [17]. Recently, Gastner et al. [23] studied a variant of the Schlögl's second model under a gradient constraint, which was called the gradient Allee process. They found that the roughness exponent that characterise the width of the MVI is given by $\alpha = 0.74 \pm 0.01$[2] and argued that a first-order percolation phase transition exists. Note that by considering $\nu_\perp = 0.35$ of the Edwards-Wilkinson (EW) universality class [22], one has that $\alpha \backsimeq 0.7407$, i.e. a figure that is fully consistent with the value reported by Gastner et al. [23]. This result suggests that the interface generated by the gradient in the Schlögl's second model [23] belongs to the EW universality class, which dominates the behaviour of the MVI at this first-order transition due to the absence of a diverging correlation length exponent. However, since the value of the roughness exponent for the KPZ universality class, which is given by $\alpha_{\rm KPZ} = 5/7 \approx 0.7143$ [17], is very close to that corresponding to the EW universality class, and since in reference [23] no finite-size corrections of the measurements are reported, one cannot outline a definitive conclusion on this issue. In Table 1 we also present a comparison between the critical parameters as obtained by using the GM and the best available values found in the literature.

Furthermore, we stress that the GM has proved to be a useful, general and efficient tool. It allows one to evaluate critical point values with very good and controlled precision, still when rather small lattices are used in the simulations. Also, it can be used to calculate the correlation length exponent of the transition under consideration. Another advantage of the GM, as follows from Table 1, is the remarkable agreement between the data obtained by means of the GM and the previously determined values obtained by using independent measurement methods. In this way, we expect that the GM will become a powerful tool for the study of far-from-equilibrium systems in statistical physics and related fields.

We acknowledge financial support from the Argentinian Science Agencies CONICET and ANPCyT, and from the UNLP (Universidad Nacional de La Plata).

References

1. J-.S. Wang, P. Nielaba, V. Privman, Physica A **199**, 527 (1993)
2. C. Fusco, P. Gallo, A. Petri, M. Rovere, J. Chem. Phys. **114**, 7563 (2001)
3. J.W. Lee, B.H. Hong, J. Chem. Phys. **119**, 533 (2003)
4. E. Eisenberg, A. Baram, J. Phys. A **30**, L271 (1997)
5. V. Pereyra, E.V. Albano, E. Duering. Phys. Rev. E **48**, R3229 (1993)
6. V. Pereyra, E.V. Albano, J. Phys. A **26**, 4175 (1993)
7. B. Bonnier, Phys. Rev. E **64**, 066111 (2001)
8. I. Lončarević, L. Budinski-Petković, S.B. Vrhovac, A. Belić, J. Stat. Mech. P02022 (2010)
9. V.A. Cherkasova, Y.Y. Tarasevich, N.I. Lebovka, N.V. Vygornitskii, Eur. Phys. J. B **74**, 205 (2010)
10. J.W. Evans, Rev. Mod. Phys. **65**, 1281 (1993)
11. V. Privman, Colloids Surf. A Physicochem. Eng. Aspects **165**, 231 (2000)
12. D. Stauffer, A. Aharoni, *Introduction to the percolation theory* (Francis and Taylor, London, 1992)
13. V. Trappe, V. Prasad, L. Cipelletti, P.N. Segre, D.A. Weitz, Nature **411**, 772 (2001)
14. A. Lawlor et al., Phys. Rev. Lett. **89**, 245503 (2002)
15. P. Olsson, S. Teitel, Phys. Rev. Lett. **99**, 178001 (2007)
16. B. Sapoval, M. Rosso, J.F. Gouyet, J. Phys. Lett. **46**, L149 (1985)
17. E.S. Loscar, N. Guisoni, E.V. Albano, Phys. Rev. E **80**, 051123 (2009)
18. N. Guisoni, E.S. Loscar, E.V. Albano, Phys. Rev. E **83**, 011125 (2011)
19. R.M. Ziff, B. Sapoval, J. Phys. A **19**, L1169 (1986)
20. N. Vandewalle, S. Galam, M. Kramer, Eur. Phys. J. B **14**, 407 (2000)
21. G. Kondrat, A. Pekalski, Phys. Rev. E **63**, 051108 (2001)
22. A.L. Barabasi, H.E. Stanley, *Fractal Concepts in Surface Growth* (Cambridge University Press, Cambridge, 1995)
23. M.T. Gastner, B. Oborny, A.B. Ryabov, B. Blasius, Phys. Rev. Lett. **106**, 128103 (2011)
24. E.S. Loscar, R.A. Borzi, E.V. Albano, Eur. Phys. J. B **36**, 157 (2003)
25. E.S. Loscar, R.A. Borzi, E.V. Albano, Phys. Rev. E **74**, 051601 (2006)
26. G. Kondrat, J. Chem. Phys. **124**, 054713 (2006)
27. V.C. Chappa, E.V. Albano, J. Chem. Phys. **121**, 328 (2004)
28. E.V. Albano, V.C. Chappa, Physica A **327**, 18 (2003)
29. R.M. Ziff, Phys. Procedia **15**, 106 (2011)
30. R.A. Monetti, E.V. Albano, Physica A **206**, 289 (1994)
31. R.A. Monetti, E.V. Albano, Chaos Solitons Fractals **6**, 379 (1995)
32. Y. Leroyer, E. Pommiers, Phys. Rev. B **50**, 2795 (1994)
33. R.M. Ziff, E. Gulari, Y. Barshad, Phys. Rev. Lett. **56**, 2553 (1986)
34. E.S. Loscar, E.V. Albano, Rep. Prog. Phys. **66**, 1343 (2003)
35. H. Hinrichsen, Adv. Phys. **49**, 815 (2000)
36. M. Kolb, Y. Boudeville, J. Chem. Phys. **92**, 3935 (1990)
37. C.A. Voigt, R.M. Ziff, Phys. Rev. E **56**, R6241 (1997)
38. E.V. Albano, Physica A **216**, 213 (1995)
39. R.M. Ziff, B.J. Brosilow, Phys. Rev. A **46**, 4630 (1992)

[2] Gastner et al. [23] have measured the interface width in lattice units, therefore the value presented for the roughnes exponent for the gradient Allee process is $\alpha^* = 0.26$. The relationship with the roughness exponent as yielded by the GM, measured in units of the control parameter, is given by $\alpha = 1 - \alpha^*$ [17].